Available online at www.sciencedirect.com

ScienceDirect

Biochimica et Biophysica Acta 1758 (2006) 1653–1661

BIOCHIMICA ET BIOPHYSICA ACTA

BBA

www.elsevier.com/locate/bbamem

Physicochemical characterization of a peptide deriving from the glycoprotein gp36 of the feline immunodeficiency virus and its lipoylated analogue in micellar systems

Cinzia Esposito [a], Gerardino D'Errico [b], Maria Rosaria Armenante [a], Simone Giannecchini [d], Mauro Bendinelli [d], Paolo Rovero [c], Anna M. D'Ursi [a,*]

[a] *Dipartimento di Scienze Farmaceutiche, Università di Salerno, via Ponte Don Melillo 11c, Fisciano, Italy*
[b] *Dipartimento di Chimica, Università di Napoli "Federico II", via Cintia, Napoli, Italy*
[c] *Laboratorio di Chimica e Biologia di Peptidi e Proteine, Dipartimento di Scienze Farmaceutiche, Università di Firenze, Sesto Fiorentino, Italy*
[d] *Centro Retrovirus e Sezione di Virologia Dipartimento di Patologia Sperimentale, Universita di Pisa, Pisa, Italy*

Received 20 January 2006; received in revised form 19 May 2006; accepted 20 June 2006
Available online 27 June 2006

Abstract

P59 is the Trp-rich 20-mer peptide (^{767}L–G^{786}), partial sequence of the membrane-proximal external region (MPER) of the FIV gp36. It has potent antiviral activity, possibly due to a mechanism that inhibits the fusion of the virus with the cell membranes. In the hypothesis that a lipophilic tail could enhance the adhesion of P59 to the membrane so improving its antiviral activity, we synthesized its lipoylated analogue lipo-P59. Fluorescence, CD and NMR investigations in membrane mimicking environments (such as SDS and DPC micelles) were aimed to assess the potential of the lipo-P59 lipophilic tail to affect the biophysical and conformational behaviour of the peptide. In vitro inhibitory assays using lymphoid cell cultures to check the antiviral activity of peptides were also performed. The data show that the biophysical properties and the conformational preferences of the peptides are not dramatically affected by the hydrophobic tail, suggesting that the lipopeptide is capable of preserving all the biophysical peculiarities. Similarly, antiviral experimental data show that the membrane-anchored lipo-P59 peptide is also effective in inhibiting virus replication. Moreover, the lipophilic tail allows P59 to preserve its antiviral activity even in conditions in which the non lipoylated peptide is devoid of activity. In accordance with the unusual high Trp presence, the peptides confirm the preference to be positioned on the membrane interface. Furthermore, the data point out a peculiarity of interaction of the peptides with SDS as compared with DPC.

Keywords: FIV; Lipopeptide; Conformational analysis; Micelle interface

1. Introduction

The feline immunodeficiency virus (FIV) is a naturally occurring lentivirus that resembles the human immunodeficiency virus (HIV) [1–4]. Much evidence suggests that FIV and HIV perform cell entry via a common molecular mechanism involving glycoproteins of the viral envelope and cell surface molecules, with the transmembrane (TM) glycoproteins gp36 and gp41, respectively, mediating the final event of membrane fusion [5–7]. Despite the low sequence homology, gp36 and gp41 exhibit a common structural framework and appear to play similar roles in virus cell fusion [8–11].

A great deal of evidence shows that a structural switching of TM glycoprotein is a key event for HIV infection. A conformational transition toward an intermediate "pre-hairpin" state favors the insertion of the hydrophobic amino-terminal fusion peptide into the target cell membrane, eventually leading to fusion [11,12].

The membrane-proximal external region (MPER) in the ectodomain of the TM glycoprotein includes an unusual clustering of triptophan residues conserved in numerous viral

* Corresponding author. Department of Pharmaceutical Sciences, University of Salerno, Via Ponte Don Melillo, 84084, Fisciano, Salerno, Italy. Tel./fax: +39 089 969748.
E-mail address: dursi@unisa.it (A.M. D'Ursi).

0005-2736/$ - see front matter © 2006 Elsevier B.V. All rights reserved.
doi:10.1016/j.bbamem.2006.06.017

enveloped TM glycoproteins, indispensable to the function of these glycoproteins [13–17]. Peptides deriving from the carboxy-terminal ectodomain of the HIV TM glycoprotein are able to prevent HIV cell membrane fusion [18–22], and one of these, known as T-20 or enfuvirtide, which includes part of the Trp-rich motif of the MPER in its C-terminus, is clinically used as an anti HIV fusion inhibitor [23].

The Trp-rich motif of FIV consists of three equally distanced Trp residues located at positions 770, 773, and 776 [24]. We recently synthesized a peptide corresponding to the ^{767}L–G^{786} sequence of gp36. This peptide, that we named P59, (LQKWEDWVGWIGNIPQYLKG) displayed antiviral activity [25]. Furthermore, on testing deleted or substituted peptides of P59, other analogues were found whose inhibitory effects were shown to be dependent on the conservation of all three Trp residues. There is enough evidence to hold that, analogously to anti-HIV fusion inhibitors, P59 and its analogues exert anti viral activity interacting with the TM glycoprotein [26].

Chemically modified peptides carrying glyco- or lipo-moieties are nowadays used for different purposes. They are held to be endowed with improved membrane permeation capabilities [27], or enhanced peptidase resistance [28]. In immunology they promote immunogenicity through better exposure to the cell surface [29]. Generally the main effect required of the lipophilic tail of the lipopeptide is an optimization of membrane adhesion [30]. However, these conjugation reactions are never devoid of side effects, since they may result in undesirable chemical and structural changes, which could lead to a decrease in biological activity [31,32].

It has been recently demonstrated that membrane anchored T20 is effective in its inhibitory action to a comparable degree to that of the free peptide [33]. In the hypothesis that effective interaction of P59 with the cell membrane surface could enhance the fusion inhibitory activity, we synthesized the P59 lipoylated analogue (lipo-P59) bearing a lipophilic tail at the C-terminus. Here, we report a combined study of P59 and its lipoylated analog aimed to asses the relation between their antiviral activity and conformational peculiarities, in particular those depending on the lipophilic tail. Hence, biological assays to check in vitro anti-FIV activity in lymphoid cell cultures were carried out. The biophysical and conformational behaviour of P59 and lipo-P59 was investigated by means of several different spectroscopic techniques, in amphiphilic systems mimicking biological membranes, such as dodecylphosphocholine (DPC) and sodium dodecyl sulphate (SDS) micelles.

2. Materials and methods

2.1. Peptide synthesis

The P59 (LQKWEDWVGWIGNIPQYLKG) peptide and its derivative containing 2-aminooctadecanoic acid (Aod) at the C-terminal, lipo-P59 (LQKWEDWVGWIGNIPQYLK(Aod)), were manually synthesized on a solid phase, using standard Fmoc/tBu chemistry. The TentaGel S RAM (0.20 mmol/g capacity) resin was purchased from Fluka (Sigma Aldrich, Italy). After deprotection of the 9-fluorenylmethoxycarbonyl (Fmoc) group with 30% piperidine in *N*,*N*-Dimethylformamide (DMF), the amino acids in 4 fold excess were coupled with the growing peptide chain, using DMF solution with an equimolar excess of 1-Hydroxybenzotriazole (HOBt) and 2-(1*H*-benzotriazol-1-yl-1,1,3,3-tetramethyluronium hexafluorophosphate (HBTU). For the synthesis of lipo-P59, the Fmoc-L-2-aminooctadecanoic acid (Fmoc-Aod-OH), from EspiKem-Italy, was introduced by a double coupling as a standard amino acid. All the reagents were from Novabiochem (France) or Sigma Aldrich (Italy); other solvents and reagents used in peptide synthesis were obtained from Sigma (Italy) or Carlo Erba (Italy) and used without further purification. Peptide–resin cleavage and side chain deprotection reactions were carried out in 95% Trifluoroacetic acid (TFA), 2.5% water and 2.5% Triisopropylsilane (TIS). After filtering to remove the resin followed by cold ether precipitation, the crude peptides were recovered, kept in aqueous solution in order to completely remove the Boc group from Trps, and lyophilized. Analytical RP-HPLC indicated a >97% purity level. Finally, the peptides were characterized on a Finningan LCQ-Deca ion trap instrument equipped with an electrospray source (LCQ Deca Finnigan, San José. CA, U.S.A.); samples were directly infused in the ESI source by using a syringe pump at the flow rate of 5 μl/min and spectra data were analyzed using Xcalibur software.

2.2. Sample preparation

Fluorescence, Circular Dichroism (CD) and Diffusion Ordered Spectroscopy (DOSY) NMR experiments were performed in SDS and DPC solutions. SDS and DPC were chosen as representatives of anionic and zwitterionic micellar systems, respectively. The measurements include general titration with surfactants starting from amounts of SDS and DPC much lower than the critical micellar concentration (cmc), to concentrations largely higher than cmc.

2.3. Fluorescence titration measurements

Peptide–surfactant interactions were studied by monitoring the changes in the Trp fluorescence emission spectra with increasing surfactant concentrations. Fluorescence measurements were performed at 300 K using a LS 55 Luminescence Spectrofluorimeter (Perkin Elmer). The excitation wavelength was 280 nm and emission spectra were recorded between 300 and 450 nm, at slit widths of 5 nm. Titrations were performed by adding measured amounts of an aqueous solution containing the peptide ($3{,}5\times10^{-5}$ M) and the surfactant at a concentration well above the cmc to a weighed amount of an aqueous solution of the peptide at the same concentration, initially put into the spectrofluorimetric cuvette. In this way, the surfactant concentration was progressively increased, while the peptide concentration remained constant during the whole titration. After each addition there was a 20-min wait to ensure equilibrium had been reached.

2.4. Circular dichroism

The peptide samples (150 μM) were prepared in a 25 mM phosphate buffer solution (pH=7), in absence and in presence of SDS or DPC surfactants, at premicellar and micellar concentrations. For micellar solutions, a 10 fold excess surfactant concentration compared to cmc was used. Peptide concentrations were estimated from the UV absorption spectra at neutral pH using a 1-cm cell (Molar absorpitivities of 5560 M^{-1} cm^{-1} and 1200 M^{-1} cm^{-1}, at 280 nm, for Triptophan and Tyrosine, respectively, were applied). CD spectra were performed on an 810-Jasco spectropolarimeter at room temperature, using a quartz cuvette with a path length of 1 mm. The spectra were the average of ten accumulations from 190 to 260 nm, recorded with a band width of 1 nm, at a scanning speed of 50 nm/min. All the spectra were analyzed, subtracted by blanks and finally corrected by smoothing. The estimation of the secondary structure composition was carried out using the algorithm K2D by Dichroweb [34].

2.5. EPR measurements

EPR characterization of micellar aggregates in the presence and in the absence of the biopeptides was performed using 5-doxylstearic acid and 16-doxylstearic acid (5-DSA and 16-DSA, respectively, Sigma products) as spin probes. The samples were prepared by weight and showed a surfactant concentration 10 times higher than cmc and a spin probe concentration equal to 0.5 mM. The concentration of the peptide, if present, was 1 mM. The samples

were deoxygenated and successively sealed in 1.00 mm i.d. quartz capillaries in a nitrogen atmosphere. EPR spectra were obtained using a Bruker ELEXYS e500 X-band spectrometer. The instrument parameters were as follows: modulation amplitude 0.16 G to avoid signal over modulation, time constant 1.28 ms, receiver gain 60 dB, microwave power 2 mW (20 dB) to prevent saturation effects. All measurements were performed at room temperature. The isotropic nitrogen hyperfine coupling constant and the correlation time of the spin probes were obtained from the experimental spectra as described in a previous work [35].

2.6. Self-diffusion experiments

NMR experiments were performed on a 600 MHz Bruker Avance spectrometer. ^{1}H NMR diffusion measurements were performed via a stimulated echo sequence with bipolar gradient pulses [36]. The diffusion time (Δ) was set to 100 ms. The pulsed gradients were increased from 2% to 95% of the maximum strength in 16 spaced steps with a duration ($\delta/2$) of 4 ms. Data were acquired in aqueous solution of ^{d25}SDS/SDS (95:5) and ^{d38}DPC/DPC (95:5) at pre-micellar and micellar concentrations. The temperature was maintained at 298 K to minimize convection effects.

2.7. FIV inhibition assay

Tests for virus inhibition were performed in 96-well flat-bottom microplates against 10 50% tissue culture infectious doses ($TCID_{50}$) of low-passage FIV-M2 isolate, using MBM cells as substrate and supernatant p25 antigen quantification as an end point, exactly as previously described [26]. Briefly, 10 $TCID_{50}$ of virus was mixed with an equal volume of the test peptides diluted from 0.0005 to 50 μg/ml (final concentrations) in a culture medium (RPMI and 10% fetal bovine serum), and immediately inoculated (100 μl/well) into 2 to 4 wells containing 10^5 MBM cells in 100 μl of culture medium. Alternatively, 10 $TCID_{50}$ of virus was inoculated into 2 to 4 wells containing 10^5 MBM cells previously pre-adsorbed with test peptides diluted from 0.0005 to 50 μg/ml at 4 °C for 1 h, centrifuged at 600×g to remove peptide and re-suspended in 100 μl of culture medium. The virus–peptide or virus-only inocula were rinsed out from the cultures after 5 h of incubation at 37 °C. After 4 days, 100 μl of supernatant was removed from each well and replaced with fresh medium. The cultures were stopped at day 8, when p25 production by control wells in which virus infection was carried out in the absence of peptide was well evident. Peptide inhibition of virus growth was calculated using the formula (mean p25 concentration in wells inoculated with FIV in presence of peptides/mean p25 concentration in wells inoculated with FIV alone)× 100. Fifty percent inhibitory concentrations (IC_{50}) were calculated using the predicted exponential growth function in Microsoft Excel as described previously. Mean IC_{50} ± Standard Deviation were calculated using all replicates. All experiments were repeated at least twice.

3. Results

3.1. Fluorescence titration measurements

The fluorescence intensities of some fine vibronic structures in the tryptophan fluorescence spectrum show strong environmental dependance [37,38]. In particular, the emission maximum shifts from 354 to 329 nm when going from water to an apolar medium. The quantum yield could also undergo large changes, the direction and extent of which depend on the system under consideration [39].

To evaluate the influence of micellar environments on the structural behaviour of P59 and lipo-P59, tryptophan fluorescence of both peptides in DPC and SDS micellar solutions was registered. The spectra are shown in Fig. 1, where they are compared with those in water. P59 in water (Fig. 1A) has a Trp emission spectrum typical of the aqueous environment (λ_{max} = 354 nm), indicating that Trps are exposed to the aqueous

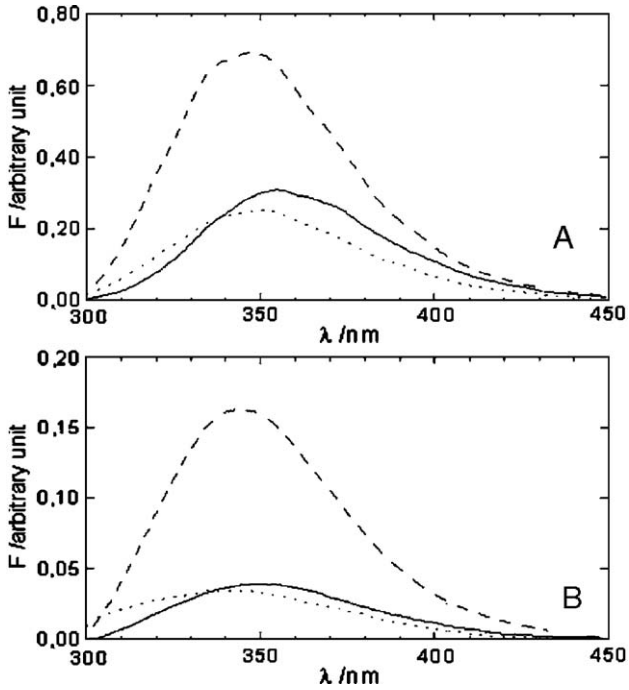

Fig. 1. Tryptophan emission spectra (range 300–450 nm) of P59 (A) and lipo-P59 (B) in aqueous buffer phosphate (unbroken line), in SDS (dotted line) and DPC (dashed line) micellar solutions.

medium. Lipo-P59 in water (Fig. 1B) has a Trp emission spectrum slightly shifted towards a lower wavelength (λ_{max} = 349 nm), suggesting that the Trps' exposure to solvent is weakly but noticeably affected by the lipoylated tail. The addition of DPC causes a change of the Trps quantum yield which could be ascribed to peptide–micelle interaction [40]. Furthermore, the spectra are slightly shifted (λ_{max} = 347 nm for P59 and λ_{max} = 343 nm for lipo-P59). The limited extent of the shift indicates that the Trps are greatly exposed to the solvent, suggesting a peptide positioning at the micelle surface rather than inside the inner hydrophobic core. Also the addition of SDS shifts the maximum of peptides spectra towards slightly lower values (λ_{max} = 350 nm for P59 and λ_{max} = 340 nm for lipo-P59), but the quantum yield change is much more limited than with DPC and in the opposite direction. Interestingly, the shift is more evident for lipo-P59, suggesting that the aliphatic chain probably favours and stabilizes the interactions of the peptide with SDS.

In order to obtain further information on peptide–surfactant interaction, Trps fluorescence of both peptides was monitored at surfactant concentrations ranging from premicellar to concentrated micellar solutions. Fig. 2A contains the variation of Trps fluorescence for both peptides at λ = 329 nm, corresponding to the emission in a hydrophobic environment, with DPC concentration. P59 and lipo-P59 display the same behaviour: in dilute surfactant solutions, fluorescence intensity is similar to that in water, indicating almost negligible interaction between both peptides and DPC monomers. At the point of micelle formation, a sharp fluorescence variation is observed, indicating involvement of the peptides in the micellar environment. As a matter of fact, the abrupt change in fluorescence occurs at a

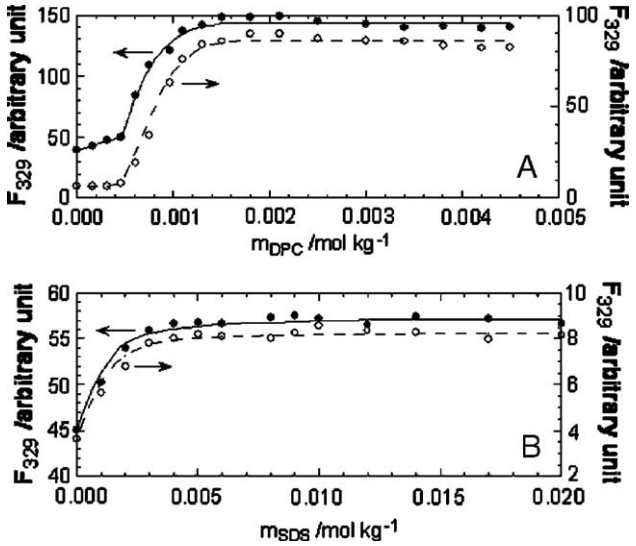

Fig. 2. Trps fluorescence variation of P59 (full circle) and lipo-P59 (empty circle) at λ=329 nm, with increasing DPC (A) and SDS (B) concentrations.

DPC concentration slightly lower than its critical micellar concentration (cmc=0.001 mol kg^{-1}), suggesting that the peptides could somehow promote surfactant aggregation.

Fig. 2B shows the variation of Trps fluorescence at λ=329 nm with SDS concentration. For both peptides, a very low amount of surfactant is sufficient to induce dramatic changes in the Trps fluorescence; moreover, no further change is observed at the point of SDS micellization (cmc=0.008 mol kg^{-1}). This evidence suggests that P59 and lipo-P59 interaction with SDS occurs with surfactant monomers rather than with micelles.

The data in Fig. 2A and B offer the opportunity for a quantification of the peptide–surfactant interaction. Actually, the quantitative description of a peptide interaction with biomembranes and related mimetic systems (vesicles, micelles) has been the subject of recent scientific discussion [41]. Two different approaches have been proposed: a partition process and a binding mechanism. In the former, a coefficient describing the mole-fraction partitioning of the peptide between the solution bulk and the microscopically dispersed hydrophobic phase, is defined as follows [42]:

$$K_{p,x} = \frac{\frac{n_{P,M}}{n_S}}{\frac{n_{P,W}}{n_W}} \quad (1)$$

where n_S and n_W are the moles of micellised surfactant and water, respectively; $n_{P,i}$ is the number of moles of peptides present in each phase (i=W, aqueous phase; i=M, micellar phase).

In the binding approach, an association constant between the peptide and the surfactant can be defined as follows [43]:

$$K_a = \frac{[PS]}{[P_F][S_F]} \quad (2)$$

where [PS] is the concentration of a peptide–surfactant complex; $[P_F]$ and $[S_F]$ are the concentrations of free peptide and free surfactant, respectively. This model can be extended to complexes formed by one peptide and n surfactant molecules.

Our experimental evidence suggests that it is not possible to decide *a priori* which one of these two approaches is correct. In fact, the partition approach well describes the systems in which aspecific solubilization of the peptide in micellar aggregates occurs, while a binding approach is preferable when direct and specific interaction between the peptide and surfactant molecules is found experimentally. In the case of fluorescence data, in the partition approach the variation of Trps fluorescence at λ=329 nm as surfactant concentration varies is expected to show a sigmoidal trend (as in the case of P59 and lipo-P59 with DPC), while in the binding approach a saturation trend is expected (as in the case of P59 and lipo-P59 with SDS).

Once the most representative model of a given system has been chosen, interpolation of the experimental Trp fluorescence data, F, by means of the proper equation allows the estimation of the $K_{p,x}$ value in the former approach, K_a and n in the latter. In fact F is a population-weighed average between the value in water, F_W, and that in micelle (or in the peptide–surfactant complex), F_M. In the partition model, this can be written as:

$$F = \frac{n_{P,W}}{n_P}F_W + \frac{n_{P,M}}{n_P}F_M \quad (3)$$

where n_P is the total number of peptide moles. Substitution of Eq. (1) in Eq. (3) yields to:

$$F = \frac{(F_M - F_W)K_{p,x}}{K_{p,x} + \frac{n_W}{n_M}} + F_W \quad (4)$$

The fitting of Eq. (4) to the experimental data allows the evaluation of $K_{p,x}$.

In the equation for the binding approach, Trp fluorescence can be expressed as:

$$F = \frac{[P_F]}{[P_{tot}]}F_W + \frac{[PS]}{[P_{tot}]}F_M \quad (5)$$

where $[P_{tot}]$ is the total concentration of peptide. Eq. (2) can be rearranged to the following quadratic equation [43]:

$$[PS]^2 - [PS]([P_{tot}] + [S_{tot}]/n + 1/nK_a) + ([S_{tot}]/n)[P_{tot}] = 0 \quad (6)$$

where $[S_{tot}]$ is the total concentration of surfactant. The solution to this quadratic equation is given by:

$$[PS] = \left\{A \pm (A^2 - 4([S_{tot}]/n)[P_{tot}])^{1/2}\right\}/2 \quad (7)$$

with

$$A = [P_{tot}] + [S_{tot}]/n + 1/nK_a \quad (8)$$

Eq. (7) has two solutions, the acceptable one being that with the positive sign. Substitution of Eq. (7) in Eq. (5) yields to the equation

$$F = \frac{(F_M - F_W)\{A + (A^2 - 4([S_{tot}]/n)[P_{tot}])^{1/2}\}/2)}{2[P_{tot}]} + F_W \quad (9)$$

that can be fitted to the experimental data so allowing us to estimate K_a and n.

Table 1 summarizes the $K_{p,x}$, K_a and n values obtained for the systems under consideration. The $K_{p,x}$ values obtained for P59 and lipo-P59 in DPC micelles are quite high, showing that both peptides tend to interact profoundly with DPC micelles. The presence of the hydrophobic chain in the lipoylated analogue does not seem to have a significant effect on the solubilization process; indeed, the $K_{p,x}$ value for lipo-P59 is slightly lower than that evaluated for P59. The K_a and n values obtained for P59 and lipo-P59 in DPC micelles show that both peptides form complexes with about 5 SDS molecules with quite a high binding constant; also in this case, the K_a value of lipo-P59 is slightly lower than that of P59.

Because of the different models used for the two surfactants, the $K_{p,x}$ and K_a values are not easily comparable, the only reasonable conclusion being that peptide–surfactant interaction occurs through different mechanisms for the two surfactants. It must be noted that the partition approach cannot be used in the case of SDS, since it would require the assumption that the surfactant cmc is null, which has no physical meaning. On the other hand, using the binding approach to data in DPC produces unsatisfactory results, since the model is not able to describe sigmoidal trends.

3.2. CD experiments

CD measurements of the two peptides were performed in a phosphate buffer (pH = 7), and in solutions containing different concentrations of SDS and DPC surfactants. As shown in Fig. 3A, in the buffer phosphate the P59 CD curve shows a prevalence of random coil conformations, whereas the lipo-P59 (Fig. 3B) CD spectrum indicates an appreciable presence of folded structures. Thus, the introduction of the hydrophobic tail seems to favor a slightly more ordered conformation in the aqueous environment.

Table 1
K_p (partitioning coefficient between the solution bulk and the microscopically dispersed hydrophobic phase), K_a (association constant between the peptide and the surfactant), and n (number of surfactant molecules interacting with the peptide), calculated for P59 and lipo-P59 in SDS and DPC micelle solutions

	$K_{p,x} \times 10^{-5}$	$K_a \times 10^{-3}$	n
H_2O-P59-DPC	3.6±0.8		
H_2O-P59-SDS		9.1±0.8	5±1
H_2O-lipo-P59-DPC	2.3±0.5		
H_2O-lipo-P59-SDS		4.2±0.9	5±2

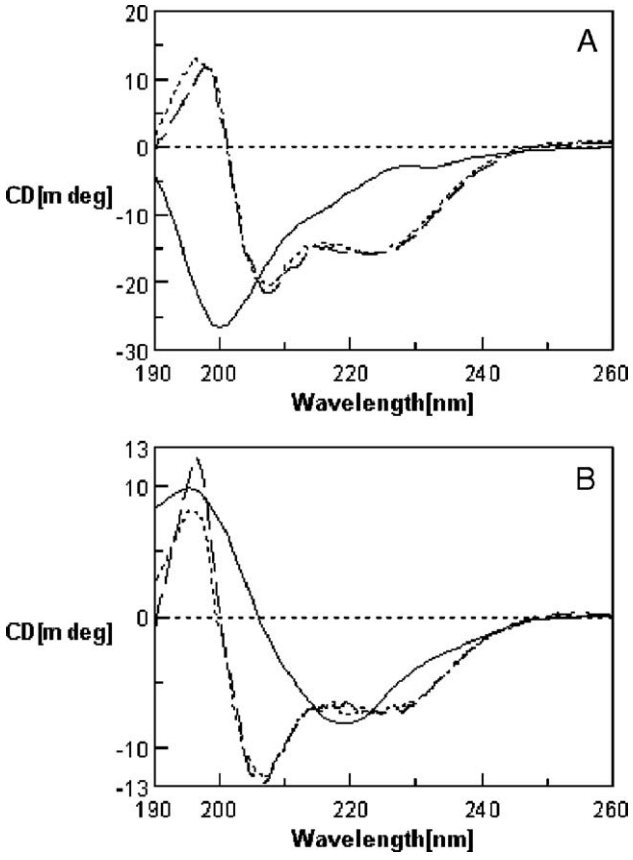

Fig. 3. CD spectra of P59 (A) and lipo-P59 (B) in aqueous buffer phosphate (unbroken line), in SDS premicellar (dotted line) and micellar (dashed line) solutions.

In SDS and DPC micellar solutions, an increase in the helical structure is observable for both peptides. In particular, in DPC micelles both peptides clearly assume an alfa-helical conformation with the two typical minima at 209 nm and 220 nm (Fig. 4).

CD spectra of P59 and lipo-P59 were also recorded in SDS and DPC surfactants in premicellar conditions. Whereas in SDS solution (Fig. 3) the transition of the CD curves from a random coil to the typical helical shape is already observable in the presence of monomers, in DPC (Fig. 4), below cmc, the CD spectra are very similar to those recorded in water solution. These results confirm the fluorescence data, suggesting an interaction between the peptides and the SDS monomers.

3.3. EPR analysis

To see whether the interaction of lipo-P59 with DPC and SDS micelles influenced the micellar structure, we performed EPR measurements on DPC and SDS micellar solutions ($m_S \approx 10$ cmc), in the absence and in the presence of the peptide, using 5-doxylstearic acid (5-DSA) and 16-doxylstearic acid (16-DSA) as spin probes [44,45]. The former provides information on the micellar layer just below the external surface, while the latter gives information on the interior of the micellar hydrophobic core. The identity of all the recorded spectra concerning the two peptides in both DPC and SDS micellar systems with 5-and 1-doxyl-stearic acids indicated no

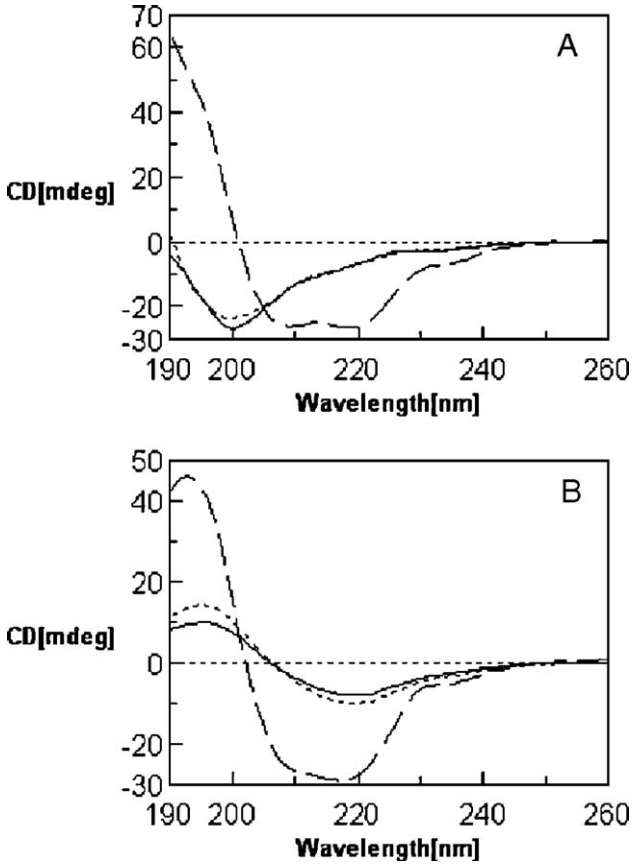

Fig. 4. CD spectra of P59 (A) and lipo-P59 (B) in aqueous phosphate buffer (unbroken line), in DPC premicellar (dotted line) and micellar (dashed line) solutions.

noticeable perturbation of the micelles. Table 2 contains the nitrogen coupling constant, indicative of microenvironment polarity, and the spin probe correlation time, indicative of microenvironment viscosity, for all the samples under consideration. Both parameters are almost unaffected by the presence of lipo-P59, showing the structure of the micellar aggregates to be unperturbed. This evidence suggests that, despite the addition of the lipoylated tail, the peptide is positioned close to the micellar surface, with very limited intrusion into the hydrophobic inner core.

3.4. Self-diffusion measurements

The diffusion coefficients of lipo-P59 were measured on the basis of NMR DOSY experiments at 600 mHz. The spectra were recorded at a constant peptide concentration (1 mM) and at two surfactant concentrations: the first at a concentration which is nearly half the cmc, i.e. in the absence of micellar aggregates, and the second at ten times cmc, i.e. in a rather concentrated micellar solution. As a comparison, the self-diffusion coefficients of the two surfactants, D_S, in premicellar solution in the absence of the peptide were also measured. Below cmc the DPC self-diffusion coefficient is only weakly affected by the peptide; shifting from 0.33×10^{-9} m^2 s^{-1} in the absence of lipo-P59 to 0.28×10^{-9} m^2 s^{-1} in the presence of the lipopeptide. Furthermore, under these conditions $D_{lipo\text{-}59}$ (0.11×10^{-9} m^2 s^{-1}) is very different from D_S, indicating negligible interaction between the two solutes. Above cmc, D_S and $D_{lipo\text{-}59}$ (0.089 10^{-9} m^2 s^{-1}) assume the same level, coincident with the self-diffusion coefficient of DPC micelles [46], thus indicating a strong association of the peptide with the DPC micellar aggregates. In the presence of SDS a quite different pattern of behaviour is observed: below cmc, the SDS self-diffusion coefficient significantly decreases from 0.49×10^{-9} m^2 s^{-1} to 0.11×10^{-9} m^2 s^{-1} because of the presence of the lipo-59, suggesting that surfactant–peptide interaction takes place. However, the mobility of the lipo-P59–SDS complex, as measured by the peptide self-diffusion, is 0.083×10^{-9} m^2 s^{-1} and thus higher than that of SDS micelles ($\sim0.052\times10^{9}$ m^2 s^{-1}) [47], suggesting that the interaction occurs between lipo-P59 and SDS monomers.

From a quantitative point of view, self-diffusion data allow us to estimate the number of SDS molecules associated to each lipo-P59 molecule in the premicellar composition range. In fact, the experimental D_S is a population-weighted average of the self-diffusion coefficients of free and bound SDS molecules, $D_{S,F}$ and $D_{S,B}$, according to the equation:

$$D_S = p_F D_{S,F} + p_B D_{S,B} \quad (10)$$

where p_F and p_B are the fractions of free and bound SDS molecules, respectively. $D_{S,F}$ can be assumed to be the same as measured in the absence of the peptide, while $D_{S,B}$ is the peptide self-diffusion coefficient. Consequently, Eq. (9) allows us to estimate the amount of free and bound SDS molecules in the sample. Under the reasonable assumption that all the peptide molecules interact with the surfactant, the ratio between the concentration of bound SDS molecules and that of the peptide gives an estimation of the number of SDS molecules bound to each lipo-P59 molecule, which was found to be ~4, in close agreement with the value obtained from fluorescence measurements.

Above cmc, D_S and $D_{lipo\text{-}59}$ are at the same level and equal to the diffusion coefficients of SDS micelles, thus indicating strong association of the peptide with SDS micellar aggregates.

3.5. Antiviral assay

To investigate on the lipophilic tail's ability to affect P59 antiviral activity, P59 and lipo-P59 were tested for their inhibitory activity on FIV replication as reported elsewhere [26]. Biological tests show that IC_{50} of P59 and lipo-P59

Table 2
Nitrogen coupling constant, and spin probe correlation time, measured by EPR experiments on P59 and lipo-P59 in SDS and DPC micelle systems

	5-DSA		16-DSA	
	$\langle A_N\rangle$/G	$\tau_C\times10^{11}$/s	$\langle A_N\rangle$/G	$\tau_C\times10^{11}$/s
H_2O-DPC	14.8	2.8	14.9	1.1
H_2O-lipo-P59-DPC	14.7	2.6	15.0	1.3
H_2O-SDS	15.6	8.2	15.4	4.7
H_2O-lipo-P59-SDS	15.4	8.4	15.2	4.5

Table 3
Inhibition of a primary FIV-M2 isolate replication by peptide 59 and lipo-59

Expt no. [a]	Mean IC_{50}±SD (μg/ml) of peptide		
	P59	lipo-P59	Control [b]
1	0.06±0.01	0.08±0.02	>50
2	>50	0.74±0.04	>50

[a] In experiment 1 the antiviral activity of the synthetic peptides was assayed for inhibition of FIV replication by the standard procedure (26). In experiment 2, aimed at checking peptide inhibitory activity adsorbed onto cell substrate, the synthetic peptides were pre-incubated with MBM cells at 4 °C for 1 h. Then the MBM cells were centrifuged at 600×g for 15 min (to remove peptides), inoculated with virus and assayed for inhibition of the FIV. The experiment was repeated three times with comparable results. IC_{50}, 50% inhibitory concentration.

[b] A 20-mer control peptide derived from a different region of the FIV TM.

(Table 3) are comparable (IC_{50} of 0.06 μg/ml and 0.08 μg/ml for peptide P59 and lipo-P59, respectively) when both peptides were mixed with virus and immediately inoculated into an MBM cell substrate. Conversely, when the peptides were pre-incubated with substrate cells and washed out by centrifugation prior to virus addition, the lipoylated analog lipo-P59 maintained a substantial antiviral activity whereas P59 was shown to be completely inactive. A 20-mer control peptide derived from a different region of the FIV TM was devoid of activity. Furthermore, peptides P59 and lipo-P59 had no detectable effects on MBM cell viability and proliferation (data not shown).

4. Discussion

P59 is the Trp-rich 20-mer peptide (^{767}L–G^{786}) derived from the MPER of the FIV gp36. Much evidence suggests that, in analogy with HIV cell entry, the TM glycoprotein plays a crucial role in the conformational arrangements leading to the fusion of FIV and cell membranes [10–12]. In particular, the MPER seems determinant for the induction and the stabilization of the conformational state preceding viral and cell membrane fusion [10,11,16,17]. Recently, it has been shown that P59 has potent antiviral activity [25]. As with HIV fusion inhibitors, it has been supposed that the P59 inhibitory mechanism could involve interaction with an as yet unidentified domain of gp36 most likely located in the N-terminus in a structural state for which membrane proximity could be a determining factor [26].

To enhance HIV antiviral activity, the expression of a membrane-anchored TM glycoprotein derived peptide has been recently carried out [33]. In the hypothesis that a lipophilic tail could enhance the adhesion of P59 to the membrane, increasing its antiviral activity, we synthesized its lipoylated analogue lipo-P59. Fluorescence, CD and NMR data in membrane mimicking environments were collected to explore solvent exposure properties and conformational preferences both in P59 and lipo-P59. The aim of the work was to assess the potential of the lipo-P59 lipophilic tail to affect biological functionality as a consequence of a modified biophysical and conformational behaviour of the peptide.

Antiviral assays showed that lipo-P59 effectively inhibits FIV replication as well as P59. Furthermore, differently from P59, it maintains its activity when it is membrane-anchored. The latter finding could most likely depend upon more effective interaction of the lipoylated peptide as compared to the non lipoylated one.

As membrane mimetics, we chose SDS and DPC micellar solutions. Since SDS and DPC are anionic and zwitterionic surfactants, respectively, they allowed us to evaluate the contribution of electrostatic and hydrophobic forces in peptide/micelle interactions.

Trp fluorescence emission spectra of P59 and lipo-P59 in water are typical of water exposed molecules whenever lipo-P59 shows to be weakly, but noticeably, affected by the lipoylated tail. This suggests that in an aqueous environment the lipophilic tail is folded toward the Trp residues, inducing the presence of a more hydrophobic environment. In the presence of increasing amounts of DPC and SDS no evidence of peptide internalization into the micelles is observable, confirming a tendency of the Trp rich fragments to be positioned at the micelle surface rather than inside the inner hydrophobic core. Furthermore whereas the interaction of P59 and lipo-P59 takes place with DPC micellar surface, a contact of the peptides with monomeric SDS results evident. It can be quantitatively estimated that about five SDS monomers interact with each peptide molecule. The peptide–SDS monomer interaction is confirmed by the NMR DOSY experiments which show a decreasing of the diffusion coefficient relative to SDS–peptide complex even at SDS concentrations much lower than cmc. On the contrary, DPC molecules and lipo-P59 have separate diffusion coefficients below cmc, assuming a unique, significantly lower diffusion coefficient when the DPC micelles are formed and the peptides interact with them. In fluorescence experiments, lipo-P59 in SDS shows the capability of the aliphatic chain to promote a more compact structure of the peptide–SDS complex. However, computed partition coefficients indicate that the aliphatic chain does not significantly affect the strength of the peptide–surfactant binding.

The conformational behaviour of P59 and its lipoylated analogue was explored by CD spectroscopy. In accordance to the fluorescence data, in water, the CD spectra of P59 and lipo-P59 point out the ability of lipo-P59 lipophilic tail to affect the conformational preference of the lipo-peptide by folding the hydrophobic chain towards the backbone. In the presence of DPC and SDS micelle solutions, P59 and lipo-P59 undergo to conformational transition resulting in a prevalence of helical structures, highlighting the ability of the membrane mimicking environment to promote a helical ordered conformation for both the peptides. Consistently with the previously mentioned spectroscopic data, the structure stabilizing effect is mediated by SDS even in monomeric state, whereas it requires DPC in micellar state.

To sum up, the reported data show that the aliphatic chain allows P59 to preserve its antiviral activity even in conditions in which the non lipoylated peptide is devoid of activity . This result can be ascribed to an enhanced interaction of lipo-P59 with the plasma membrane compared to P59, most likely

leading to a high local concentration of peptide in the site of its action. Hence, it is interesting to observe that the biophysical properties and the conformational preferences of the peptides are not dramatically affected by the lipophilic tail, suggesting that the lipopeptide has the capability to preserve all the biophysical characteristics.

Furthermore, our study has highlighted the importance of the choice of membrane mimicking systems used in biological research. In fact, SDS and DPC interact in different ways with our peptides, leading to formulate new hypotheses on the dynamic of interaction between bio-molecules and different surfactants. In particular, the dynamic of aggregation of our peptides with SDS monomers suggests a mechanism of surfactant interaction, in which the peptides can work as starter of micelle formation. The process should be triggered by a hydrophobic interaction between the hydrophobic portion of the peptides and the lipophilic tails of SDS detergent. Synergistically, the SDS–peptide contact is stabilized by an electrostatic interaction occurring between the strongly negative headgroups of SDS and the positive side chains of lysines, which are present in the extremities of the P59 sequence. On the contrary, in DPC solution the peptides seem to be not involved in the process of micelle formation, probably due to the limited stabilizing electrostatic interaction with the zwitterionic headgroups. Thus, the micelle formation seems to occur independently than the presence of the peptides which show to have contact just with the micelle surface of the surfactant.

References

[1] N.C Pedersen, E.W. Ho, M.L. Brown, J.K. Yamamoto, Isolation of a T-lymphotropic virus from domestic cats with an immunodeficiency-like syndrome, Science 235 (1987) 790–793.

[2] J.H. Elder, T.R. Phillips, Feline immunodeficiency virus as a model for development of molecular approaches to intervention strategies against lentivirus infections, Adv. Virus Res. 45 (1995) 225–247.

[3] T. Lee, G.S. Laco, B.E. Torbett, H.S. Fox, D.L. Lerner, J.H. Elder, C.H. Wong, Analysis of the S3 and S3′ subsite specificities of feline immunodeficiency virus (FIV) protease: development of a broad-based protease inhibitor efficacious against FIV, SIV, and HIV in vitro and ex vivo, Proc. Natl. Acad. Sci. U. S. A. 95 (1998) 939–944.

[4] B.J. Willett, J.N. Flynn, M.J. Hosie, FIV infection of the domestic cat: an animal model for AIDS, Immunol. Today 18 (1997) 182–189.

[5] A. de Parseval, C.K. Grant, K.J. Sastry, J.H. Elder, Sequential CD134–CXCR4 interactions in feline immunodeficiency virus (FIV): soluble CD134 activates FIV Env for CXCR4-dependent entry and reveals a cryptic neutralization epitope, J. Virol. 80 (2006) 3088–3091.

[6] S.C. Frey, E.A. Hoover, J.I. Mullins, Feline immunodeficiency virus cell entry, J. Virol. 75 (2001) 5433–5440.

[7] R. Wyatt, J. Sodroski, The HIV-1 envelope glycoproteins: fusogens, antigens, and immunogens, Science 280 (1998) 1884–1888.

[8] G. Pancino, L. Camoin, P. Sonigo, Structural analysis of the principal immunodominant domain of the feline immunodeficiency virus transmembrane glycoprotein, J. Virol. 69 (1995) 2110–2118.

[9] P.F. Serres, Molecular mimicry between the trimeric ectodomain of the transmembrane protein of immunosuppressive lentiviruses (HIV–SIV–FIV) and interleukin 2, C. R. Acad. Sci. III 323 (2000) 1019–1029.

[10] S. Giannecchini, F. Bonci, M. Pistello, D. Matteucci, O. Sichi, P. Rovero, M. Bendinelli, The membrane-proximal tryptophan-rich region in the transmembrane glycoprotein ectodomain of feline immunodeficiency virus is important for cell entry, Virology 320 (2004) 156–166.

[11] D.C. Chan, P.S. Kim, HIV entry and its inhibition, Cell 93 (1998) 681–684.

[12] R.W. Doms, J.P. Moore, HIV-1 membrane fusion: targets of opportunity, J. Cell Biol. 151 (2000) 9–14.

[13] T. Suarez, W.R. Gallaher, A. Agirre, F.M. Goni, J.L. Nieva, Membrane interface-interacting sequences within the ectodomain of the human immunodeficiency virus type 1 envelope glycoprotein: putative role during viral fusion, J. Virol. 74 (2000) 8038–8047.

[14] T. Suarez, S. Nir, F.M. Goni, A. Saez-Cirion, J.L. Nieva, The pre-transmembrane region of the human immunodeficiency virus type-1 glycoprotein: a novel fusogenic sequence, FEBS Lett. 477 (2000) 145–149.

[15] S.G. Peisajovich, L. Blank, R.F. Epand, R.M. Epand, Y. Shai, On the interaction between gp41 and membranes: the immunodominant loop stabilizes gp41 helical hairpin conformation, J. Mol. Biol. 326 (2003) 1489–1501.

[16] K. Salzwedel, J.T. West, E. Hunter, A conserved tryptophan-rich motif in the membrane-proximal region of the human immunodeficiency virus type 1 gp41 ectodomain is important for Env-mediated fusion and virus infectivity, J. Virol. 73 (1999) 2469–2480.

[17] D.J. Schibli, R.C. Montelaro, H.J. Vogel, The membrane-proximal tryptophan-rich region of the HIV glycoprotein, gp41, forms a well-defined helix in dodecylphosphocholine micelles, Biochemistry 40 (2001) 9570–9578.

[18] H. Ji, W. Shu, F.T. Burling, S. Jiang, M. Lu, Inhibition of human immunodeficiency virus type 1 infectivity by the gp41 core: role of a conserved hydrophobic cavity in membrane fusion, J. Virol. 73 (1999) 8578–8586.

[19] B. Jin, S. Jin, R. Ryu, K. Ahn, Y.G. Yu, Design of a peptide inhibitor that blocks the cell fusion mediated by glycoprotein 41 of human immunodeficiency virus type 1, AIDS Res. Hum. Retroviruses 16 (2000) 1797–1804.

[20] J.K. Judice, Y. Judice, K. Tom, W. Huang, T. Wrin, J. Vennari, C.J. Petropoulos, R.S. McDowell, Inhibition of HIV type 1 infectivity by constrained α-helical peptides: implications for the viral fusion mechanism, Proc. Natl. Acad. Sci. USA 94 (1997) 13426–13430.

[21] C.T. Wild, D.C. Shugars, T.K. Greenwell, C.B. McDanal, T.J. Matthews, Peptides corresponding to a predictive α-helical domain of human immunodeficiency virus type 1 gp41 are potent inhibitors of virus infection, Proc. Natl. Acad. Sci. U. S. A. 91 (1994) 9770–9774.

[22] A.R. Neurath, K. Lin, N. Strick, S. Jiang, Multifaceted consequences of anti-gp41 monoclonal antibody 2F5 binding to HIV type 1 virions, AIDS Res. Hum. Retrovir. 11 (1995) 687–696.

[23] J.M. Kilby, J.P. Lalezari, J.J. Eron, M. Carlson, C. Cohen, R.C. Arduino, J.C. Goodgame, J.E. Gallant, P. Volberding, R.L. Murphy, F. Valentine, M.S. Saag, E.L. Nelson, P.R. Sista, A. Dusek, The safety, plasma pharmacokinetics, and antiviral activity of subcutaneous enfuvirtide (T-20), a peptide inhibitor of gp41-mediated virus fusion, in HIV-infected adults, AIDS Res. Hum. Retrovir. 18 (2002) 685–693.

[24] R.L. Talbott, E.E. Sparger, K.M. Lovelace, W.M. Fitch, N.C. Pedersen, P.A. Luciw, J.H. Elder, Nucleotide sequence and genomic organization of feline immunodeficiency virus, Proc. Natl. Acad. Sci. U. S. A. 86 (1989) 5743–5747.

[25] S. Lombardi, C. Massi, E. Indino, C. La Rosa, P. Mazzetti, M.L. Falcone, P. Rovero, A. Fissi, O. Pieroni, P. Bandecchi, F. Esposito, F. Tozzini, M. Bendinelli, C. Garzelli, Inhibition of feline immunodeficiency virus infection in vitro by envelope glycoprotein synthetic peptides, Virology 220 (1996) 274–284.

[26] S. Giannecchini, A. Di Fenza, A.M. D'Ursi, D. Matteucci, P. Rovero, M. Bendinelli, Antiviral activity and conformational features of an octapeptide derived from the membrane-proximal ectodomain of the feline immunodeficiency virus transmembrane glycoprotein, J. Virol. 77 (2003) 3724–3733.

[27] I. Toth, N. Flinn, A.M. Hillery, W.A. Gibbons, P. Artursson, Lipidic conjugates of LHRH and TRH that release and protect the native hormones in homogenates of human intestinal epithelial (Caco-2) cells, Int. J. Pharm. 105 (1994) 241–247.

[28] I. Toth, A novel chemical approach to drug delivery: lipidamino acid conjugates, J. Drug Target. 2 (1994) 217–239.
[29] I. Toth, M. Danton, N. Flinn, A.M. Hillery, I.P. Wood, W.A. Gibbons, A lipidic α-amino acid-based synthetic adjuvant peptide complex for increasing immunogenicity of vaccines, Biochem. Soc. Trans. 22 (1994) 1055–1058.
[30] R.M. Epand, Biophysical studies of lipopeptide–membrane interactions, Biopolymers 43 (1997) 15–24.
[31] Ka-yun Ng, L. Zhao, J.D. Meyer, L. Rittmann-Grauer, M.C. Manning, Use of circular dichroism spectroscopy in determining the conformation of a monoclonal antibody prior to its incorporation in an immunoliposome, J. Pharm. Biomed. Anal. 16 (1997) 507–513.
[32] R. Romano, H.J. Musiol, E. Weyher, M. Dufresne, L. Moroder, Peptide hormone–membrane interactions: the aggregational and conformational state of lipo-gastrin derivatives and their receptor binding affinity, Biopolymers 32 (1992) 1545–1558.
[33] M. Egelhofer, G. Brandenburg, H. Martinius, P. Schult-Dietrich, G. Melikyan, R. Kunert, C. Baum, I. Choi, A. Alexandrov, D. von Laer, Inhibition of human immunodeficiency virus type 1 entry in cells expressing gp41-derived peptides, J. Virol. 78 (2004) 568–575.
[34] L. Whitmore, B.A. Fallace, DICHROWEB, an online server for protein secondary structure analysis from circular dichroism spectroscopic data, Nucleic Acids Res. 32 (2004) 668–673.
[35] A.M. Tedeschi, L. Franco, M. Ruzzi, L. Padano, C. Corvaja, G. D'Errico, Micellar aggregation of alkyltrimethylammonium bromide surfactants studied by electron paramagnetic resonance of an anionic nitroxide, Phys. Chem. Chem. Phys. 5 (2003) 4204–4209.
[36] C.S. Johnson Jr., Diffusion ordered nuclear magnetic resonance spectroscopy principles and applications, Prog. NMR Spectrosc. 34 (1999) 203–256.
[37] S.V. Konev, Fluorescence and Phosphorescence of Proteins and Acids, Plenum, New York, 1967.
[38] L. Ambrosone, G. D'Errico, R. Ragone, Interaction of tryptophan and N-acetyltryptophanamide with dodecylpentaoxyethyleneglycol ether micelles, Spectrochim. Acta 53 (1997) 1615–1620.
[39] P.R. Callis, T. Liu, Quantitative prediction of fluorescence quantum yields for tryptophan in proteins, J. Phys. Chem., B 108 (2004) 4248–4259.
[40] J. Dufourcq, J.F. Faucon, R. Maget-Dana, M.P. Pileni, C. Helene, Peptide–membrane interactions. A fluorescence study of the binding of oligopeptides containing aromatic and basic residues to phospholipid vesicles, Biochim. Biophys. Acta, Biomembr. 649 (1981) 67–75.
[41] N.C. Santos, M. Prieto, M.A. Castanho, Quantifying molecular partition into model systems of biomembranes: an emphasis on optical spectroscopic methods, Biochim. Biophys. Acta 1612 (2003) 123–135.
[42] W. Nernst, Verteilung eines stoffes zwishen zwei lo¨ungsmitteln und zwishen lo¨sungsmittel und dampfraum, Z. Phys. Chem. 8 (1891) 110–139.
[43] B. Christiaens, S. Symoens, S. Verheyden, Y. Engelborghs, A. Joliot, A. Prochiantz, J. Vandekerckhove, M. Rosseneu, B. Vanloo, Tryptophan fluorescence study of the interaction of penetratin peptides with model membranes, Eur. J. Biochem. 269 (2002) 2918–2926.
[44] G.L. Mendz, W.J. Moore, I.J. Kaplin, B.A. Cornell, F. Separovic, D.J. Miller, L.R. Brown, Characterization of dodecylphosphocholine/myelin basic protein complexes, Biochem. 27 (1988) 379–386.
[45] Y.S. Kang, L. Kevan, Interaction of Poly(ethylene oxide) with sodium dodecyl sulfate micelle interface studied with nitroxide spin probes, J. Phys. Chem. 98 (1994) 7624–7627.
[46] D.A. Kallick, M.R. Tessmer, C.R. Watts, C.Y. Li, The use of dodecylphosphocholine micelles in solution NMR, J. Magn. Reson., Ser. B 109 (1995) 60–65.
[47] S. Albrizio, G. Caliendo, G. D'Errico, E. Novellino, P. Rovero, A.M. D'Ursi, Galphas protein C-terminal alpha-helix at the interface: does the plasma membrane play a critical role in the Galphas protein functionality, J. Pept. Sci. 11 (2005) 617–626.